Modified photoluminescence properties of rare-earth complex/polymer composite fibers prepared by electrospinning

Hui Zhang, Hongwei Song, Hongquan Yu, Suwen Li, Xue Bai et al.

Citation: Appl. Phys. Lett. **90**, 103103 (2007); doi: 10.1063/1.2711380
View online: http://dx.doi.org/10.1063/1.2711380
View Table of Contents: http://apl.aip.org/resource/1/APPLAB/v90/i10
Published by the American Institute of Physics.

Modified photoluminescence properties of rare-earth complex/polymer composite fibers prepared by electrospinning

Hui Zhang, Hongwei Song,[a] Hongquan Yu, Suwen Li, Xue Bai, Guohui Pan, Qilin Dai, Tie Wang, Wenlian Li, Shaozhe Lu, Xinguang Ren, Haifeng Zhao, and Xianggui Kong
Key Laboratory of Excited State Physics, Changchun Institute of Optics, Fine Mechanics and Physics, Chinese Academy of Sciences, 16 Eastern South-Lake Road, Changchun 130033, People's Republic of China

(Received 31 August 2006; accepted 29 January 2007; published online 6 March 2007)

Efficiently luminescent composite fibers of poly (vinyl pyrrolidone) ($M_w \approx 1\,300\,000$) and europium complex $Eu(TTA)_3(TPPO)_2$ (TTA is thenoyltrifluoroacetone; TPPO is triphenylphosphine oxide) were prepared by electrospinning, with average diameters of 200–500 nm and lengths of several tens of micrometers. Their photoluminescence properties were studied in comparison to the pure $Eu(TTA)_3(TPPO)_2$ complex. It was significant to observe that the thermal stability of photoluminescence in the composite fibers was improved considerably over the pure complex.
 [DOI: 10.1063/1.2711380]

Lanthanide complexes have long been known to give sharp, intense emission lines upon ultraviolet light irradiation, because of the effective intramolecular energy transfer from the coordinated ligands to the luminescent central lanthanide ions, which in turn undergo the corresponding radiative emitting process (the so-called antenna effect).[1] However, the lanthanide complexes suffer low mechanical strength, poor thermal stability, and low resistance to moisture, which make them unsuitable for applications. In order to overcome these problems, some work has been done to disperse lanthanide complexes into polymer and inorganic matrices.[2–6] The development of organic-inorganic hybrid materials has been the subject of extensive research in the past decade because these systems are found to have the advantage in many fields of applications as they combine both inorganic and organic characters.[7–11]

One-dimensional (1D) nanostructures have attracted much attention in recent years due to their importance for both fundamental studies and technological applications.[12] A large number of synthetic and fabrication methods have already been demonstrated for generating 1D nanostructures in the form of fibers, wires, rods, belts, tubes, spirals, and rings from various materials.[13] Among these methods, electrospinning has attracted rapidly increasing attention as a simple physical method for generating nanofibers. As a nonmechanical fiber drawing method, electrospinning involves the stretching of a polymer solution (or melt) with electrostatic forces. Electrospinning requires the use of an appropriate solvent and polymer system to prepare solutions exhibiting the desired viscoelastic behavior.

In this study, $Eu(TTA)_3(TPPO)_2$/PVP composite fibers with intense brightness were prepared through electrospinning [TTA is thenoyltrifluoroacetone, TPPO is triphenylphosphine oxide, and PVP is poly (vinyl pyrrolidone)]. Their luminescence properties were studied in comparison to that of the relevant pure europium complex. It is important to observe that the temperature dependence of the luminescence in the composite fibers was considerably improved over the pure europium complex below room temperature.

$Eu(TTA)_3(TPPO)_2$ was synthesized according to the traditional method.[14] In the preparation of composite fibers, an appropriate amount of PVP was dissolved in 10 ml ethanol solution at concentrations of 7, 9, and 12 wt %, respectively. After stirring, $Eu(TTA)_3(TPPO)_2$ with the same weight was dissolved, respectively, into the prepared 7, 9, and 12 wt % PVP ethanol solutions, corresponding to the mass ratios of $Eu(TTA)_3(TPPO)_2$ complex to PVP of 1:23, 1:30, and 1:40. They were stirred to be uniform. The final solutions then were electrospun to be composite fibers of $Eu(TTA)_3(TPPO)_2$ complex and PVP. The schematic diagram of the electrospinning setup is drawn in Fig. 1. It consists of three major components: a high-voltage power supply, a spinneret (a needle), and a collector plate (a grounded conductor). The voltage used for electrospinning was 14 kV. In the following text, the pure $Eu(TTA)_3(TPPO)_2$ complex and $Eu(TTA)_3(TPPO)_2$/PVP composite fibers electrospun

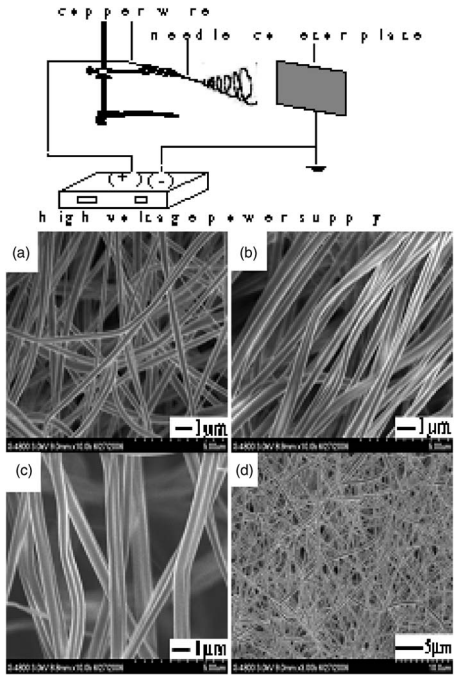

FIG. 1. Schematic diagram of the electrospinning setup and the SEM images of $Eu(TTA)_3(TPPO)_2$/PVP composite fibers: (a) sample B, (b) sample C, and (c) sample D. (d) Image for sample C in a large scale.

[a]Author to whom correspondence should be addressed; FAX: 86-431-86176320; electronic mail: hwsong2005@yahoo.com.cn

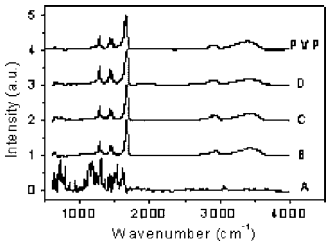

FIG. 2. Infrared absorption spectra of the pure $Eu(TTA)_3(TPPO)_2$ complex (sample A), the $Eu(TTA)_3(TPPO)_2$/PVP composite fibers (samples B, C, and D) and the pure PVP fibers.

from 7, 9, and 12 wt % concentrations of PVP ethanol solution are labeled as samples A, B, C, and D, respectively.

The size and morphology of the composite fibers were obtained by using an S-4800 scanning electron microscope (Hitachi). The excitation and emission spectra were recorded at room temperature using a Hitachi F-4500 spectrophotometer. In the measurements of the temperature dependence of photoluminescence the samples were placed in a liquid nitrogen cycling system (pellet). A continuous 325 nm light from a He–Cd laser was used as excitation source. The fluorescence was measured by an UV-Lab Raman Infinity (made by Jobin Yvon Company) with a resolution of 2 cm^{-1}. In the measurements of fluorescence dynamics, a 355 nm light generated from a Nd^{3+}:YAG (yttrium aluminum garnet) pulsed laser combined with a third-harmonic generator was used as pumping. An oscillograph was used to record the decay dynamics. The refractive indices of TTA and TPPO were measured by a spectroscopic ellipsometer (Jobin Yvon HORIBA).

Figures 1(a)–1(c) show the scanning electron microscope (SEM) image of fiber composite samples B, C, and D, respectively. It can be seen that the average diameters for the three samples are ~200, 400, and 500 nm, respectively. Apparently, the diameters of the composite fibers increase with the increase of PVP concentration. Figure 1(d) displays that uniform and superlong nanowires are formed in sample C, with lengths of several tens to hundreds of micrometers. The composite fibers in the other samples yield similar lengths.

Figure 2 shows the Fourier transform infrared (FTIR) spectra of the different samples. The $Eu(TTA)_3(TPPO)_2$ complex used to fabricate the composite fibers is a kind of nonhydrated complex, which can be proven by the absence of O–H stretching mode in the IR absorption spectrum for the pure $Eu(TTA)_3(TPPO)_2$ complex. The composite fibers contain trace hydroxyl group due to the electrospun solution. A broad band at 3400 cm^{-1} appears in the composite fibers, which is assigned to vibration of the associated hydroxyl groups. The FTIR spectra of the composite fibers are similar to that of the PVP fibers electrospun from the PVP ethanol solution, suggesting that the europium complexes are capped in the PVP matrix in the composite fibers.

The photoluminescence properties of the composite fibers were studied and compared with that of the pure europium complex. Figure 3(a) shows the photographs of the different samples under the irradiation of the 365 nm Hg lamp. From Fig. 3(a) we can see that the brightness of the composites is very intense, although the concentration of the europium complex in the samples is quite little. The photoluminescence quantum efficiencies of samples A, B, C, and D measured by the integrating sphere method were 67.3%, 52.8%, 51.2%, and 49.2%, respectively. The little decrease of quantum efficiency in the composites may be caused by

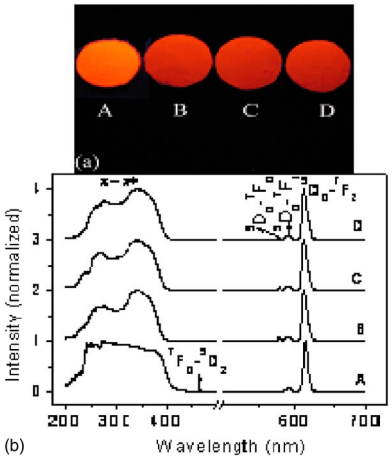

FIG. 3. (Color online) (a) Photographs of the different samples under the irradiation of 365 nm Hg lamp. (b) Excitation spectra (λ_{em}=611 nm) and emission spectra (λ_{ex}=340 nm) for the $^5D_0$-^7F_J transitions of Eu^{3+} in the different samples.

the influence of the hydroxyl group involved in the preparation. Figure 3(b) shows the excitation and emission spectra of various samples. In the pure complex, a broad excitation band extending from 200 to 400 nm appears, which is assigned to the π-π^* electron transition of the ligands. In the composite, it is interesting to observe that the excitation band is split into two components, having peaks at ~260 and ~340 nm, respectively. This indicates that in the composite due to the existence of the surrounding PVP media, the site symmetry becomes lower.[15] In addition, in the excitation spectrum of the pure complex the $^7F_0$-$^5D_2$ excitation line appears, while in the composites the line disappears. This suggests that in the composites the *f*-*f* inner-shell transitions are completely quenched through the nonradiative energy transfer from the higher excited states to some uncertain defect levels, substituting for the nonradiative relaxation from higher excited states to $^5D_0$.

In the emission spectra, the red $^5D_0$-^7F_J (J=0,1,2) transitions are clearly observed. The emission lines in the composites become broader over the pure complex, which is attributed to heterogeneous broadening caused by more disordered local environments surrounding Eu^{3+} ions.

The fluorescence decay curves of $^5D_0$-$^7F_2$ emissions for Eu^{3+} under 355 nm excitation were measured at room temperature, as shown in Fig. 4. It can be seen that the fluorescence decays exponentially for all the samples. The exponential lifetimes for the $^5D_0$ states are obtained to be 450 μs in sample A, 554 μs in sample B, 520 μs in sample C, and 500 μs in sample D. It is obvious that the fluorescence lifetime for the $^5D_0$ state in the composite fibers becomes longer than that in the pure europium complex.

In fact, the lifetime of $^5D_0$, τ, is dominated by the total radiative transition rate of $^5D_0$-Σ ^7F_J, W_r, and the nonradia-

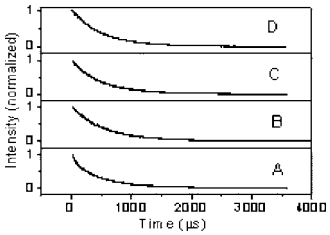

FIG. 4. Fluorescence decay dynamics of the $^5D_0$-$^7F_2$ transitions (λ_{em}=614 nm) in various samples (room temperature).

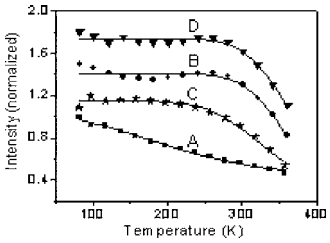

FIG. 5. Dependence of emission intensity of the $\Sigma\,{}^5D_0$-${}^7F_J$ transitions on temperature.

tive decay rate W_{nr}, which can be written as $\tau=[1/(W_r+W_{nr})]$. W_{nr} includes the nonradiative relaxation rate from ${}^5D_0$ to lower ${}^7F_J$ levels and nonradiative energy transfer rate to the other defect centers. Generally, the nonradiative transition rate increases strongly with temperature, while the radiative transition rate is nearly independent of temperature. By measuring the temperature dependence (10–300 K), we determined that the fluorescence lifetime of ${}^5D_0$ had little variation on temperature, which implied that the nonradiative relaxation rate could be neglected below room temperature and the lifetime was dominated by the radiative transition rate.[16]

In the composite, the refractive index surrounding Eu^{3+} ions has changed in comparison to the pure complex, which should have influence on the radiative fluorescence lifetime of Eu^{3+}. The radiative lifetime can be written as

$$\tau_R \approx \frac{1}{f(\mathrm{ED})}\frac{\lambda_0^2}{[(1/3)(n^2+2)]^2 n}, \tag{1}$$

where f(ED) is the oscillator strength for the electronic dipole transition, λ_0 is the wavelength in vacuum, and n is the refractive index of the material. Meltzer *et al.* observed that the radiative lifetime of Y_2O_3:Eu^{3+} nanocrystals depended not only on the refractive index itself but also on the surrounding medium. They deduced that in nanoparticles, n in Eq. (1) should be substituted by the effective index $n_{eff}=xn+(1-x)n_{med}$, where x is the filling factor showing what fraction of the space is occupied by the nanoparticles and n_{med} is the refractive index of the surrounding media.[17] In the composite, the complexes are surrounded by PVP media. The values of the refractive index are, respectively, 1.56 for TTA, 1.72 for TPPO, and 1.53 for PVP.[18] The decreased refractive index of the surrounding media (PVP) will lead n_{eff} to be smaller than n, inducing the increase of radiative lifetime.

To study the thermal stability of photoluminescence, the temperature dependence of fluorescence intensity was measured under the 325 nm excitation in various samples. Figure 5 shows the dependence of the emission intensity of ${}^5D_0$-${}^7F_2$ on temperature. It is obvious that the variation of the emission intensity for the Eu^{3+} ion in the composite fibers shows a remarkable difference related to that in the pure complex. The emission intensity of the pure $Eu(TTA)_3(TPPO)_2$ complex powder decreases monotonically with the increasing temperature in the studied range. In the $Eu(TTA)_3(TPPO)_2$/PVP composite fibers the total emission intensity of the Eu^{3+} ions changes little below the room temperature, then it decreases quickly as temperature increases continuously. In Fig. 5, the intensity as a function of temperature can be well fitted by the well-known thermal activation function[19]

$$I(T)=\frac{I}{1+\alpha e^{-E_A/K_BT}}, \tag{2}$$

where I_0 is the emission intensity at 0 K, α is the proportional coefficient, E_A is the thermal activation energy, K_B is Boltzmann's constant, and T is the absolute temperature. The values of E_A in samples A, B, C, and D are, respectively, 40.3, 344.7, 202.6, and 317.4 meV. The improved value of E_A in the composite fibers suggests that the thermal stability of the photoluminescence is much better than that in the pure complexes. We suggest that in the composites, due to the existence of PVP matrix, the vibrational transitions of the complexes were restrained, leading to improved thermal stability of photoluminescence.[20]

In summary, uniform and superlong $Eu(TTA)_3(TPPO)_2$/PVP composite fibers were prepared by electrospinning and their photoluminescence were studied. Due to the degeneration of crystal field, the excitation bands were split into different components. The fluorescence decay time constants for the ${}^5D_0$-${}^7F_2$ transitions became longer because of the influence of the surrounding refractive index. The most important is that in the composite fibers, the temperature stability of the photoluminescence became much better in comparison to the pure complex due to the modification by the PVP matrix.

The authors thank the financial support by the National Natural Science Foundation of China (Grant Nos. 10374086 and 10504030) and Talent Youth Foundation of Jilin Province (Grant No. 20040105). They also thank Dongge Ma for the help in the measurement of photoluminescence quantum efficiency.

[1] S. Sato and M. Wada, Bull. Chem. Soc. Jpn. **43**, 1955 (1970).
[2] L. R. Matthews and E. T. Knobbe, Chem. Mater. **5**, 1697 (1993).
[3] T. Kobayashi, S. Nakatsuka, T. Iwafuji, K. Kuriki, N. Imai, T. Nakamoto, C. Claude, K. Sasaki, Y. Koike, and Y. Okamoto, Appl. Phys. Lett. **71**, 2421 (1997).
[4] C. Koeppen, S. Yamada, G. Jiang, A. F. Garito, and L. R. Dalton, J. Opt. Soc. Am. B **14**, 155 (1997).
[5] T. Jin, S. Tsutsumi, Y. Deguchi, K. Machida, and G. Adachi, J. Alloys Compd. **252**, 59 (1997).
[6] S. Sato, R. Yamaguchi, and T. Nose, Trans. Inst. Electron., Inf. Commun. Eng. C-II **J72C-II**, 906 (1989).
[7] A.-C. Franville, D. Zambon, and R. Mahiou, Chem. Mater. **12**, 428 (2000).
[8] H. H. Li, S. Inoue, K.-I. Machida, and G.-Y. Adachi, Chem. Mater. **11**, 3171 (1999).
[9] B. Lintner, N. Arfsten, H. Pislich, H. Schmidt, G. Philipp, and B. Serferling, J. Non-Cryst. Solids **100**, 378 (1998).
[10] J. Wen and G. L. Wilkes, Chem. Mater. **8**, 1667 (1996).
[11] C. Sanchez and F. Babonneau, *Materiaux Hybrides; Observatoire Francais des Techniques Advancees* (Masson, Paris 1996).
[12] For a review, see Y. Xia, P. Yang, Y. Sum, Y. Wu, B. Mayers, B. Gates, Y. Yin, F. Kim, and H. Yan, Adv. Mater. (Weinheim, Ger.) **15**, 353 (2003).
[13] Adv. Mater. (Weinheim, Ger.) **15**, 351 (2003), special issue on Chemistry and Physics of Nanowires.
[14] L. R. Melby, N. J. Rose, E. Abramson, and J. C. Caris, J. Am. Chem. Soc. **86**, 5117 (1964).
[15] N. C. Chang and J. B. Gruber, J. Chem. Phys. **41**, 3227 (1964).
[16] H. S. Peng, H. W. Song, B. J. Chen, J. W. Wang, S. Z. Lu, X. G. Kong, and J. H. Zhang, J. Chem. Phys. **118**, 3277 (2003).
[17] R. S. Meltzer, S. Feofilov, and B. M. Tissue, Phys. Rev. B **60**, R14012 (1999).
[18] P. Belleville, C. Bonnin, E. Lavastre, P. Pegon, and Y. Rorato, Proc. SPIE **4347**, 588 (2001).
[19] B. S. Li, Y. C. Liu, Z. Z. Zhi, D. Z. Shen, Y. M. Lu, J. Y. Zhang, and X. W. Fan, J. Cryst. Growth **240**, 479 (2002).
[20] Q. Li, T. Li, and J. G. Wu, J. Phys. Chem. B **105**, 12293 (2001).